

“© 2019 IEEE. Personal use of this material is permitted. Permission from IEEE must be obtained for all other uses, in any current or future media, including reprinting/republishing this material for advertising or promotional purposes, creating new collective works, for resale or redistribution to servers or lists, or reuse of any copyrighted component of this work in other works.”

Low-Overhead Handover-Skipping Technique for 5G Networks

Cristo Suarez-Rodriguez
School of Electrical and Data Engineering
University of Technology Sydney
Sydney, Australia
Cristo.Suarez@student.uts.edu.au

Ying He
School of Electrical and Data Engineering
University of Technology Sydney
Sydney, Australia
Ying.He@uts.edu.au

Beeshanga A. Jayawickrama
Ericsson
beeshanga.jayawickrama@ericsson.com

Eryk Dutkiewicz
School of Electrical and Data Engineering
University of Technology Sydney
Sydney, Australia
Eryk.Dutkiewicz@uts.edu.au

Abstract—Network densification has been one of the principal causes of performance gain in cellular networks, and 5G networks will not be any different. As cell sizes shrink, handovers become more frequent incurring extra delays that bury all the prospective gains. Mobility in multi-tier dense cellular networks calls for a change in the way it has been traditionally handled in an always-on world, where users take universal data access for granted. Invisible to them, mobile network operators need to provision backhauling to include advanced interference mitigation techniques. In this paper, we propose a spectrum database-aided handover management technique that aims to mitigate the number of disconnections without overloading the backhaul unnecessarily. The proposed technique exploits a spectrum database that stores reception information along with geolocation data, commercially available on any handheld device. Moreover, we have benchmarked several state-of-the-art handover schemes for 5G networks against ours in a realistic urban environment with user mobility trace data. The results highlight that our method can deliver the same downstream traffic with 33% decrease in disconnections when compared to the conventional approach. At the same time, backhaul traffic is reduced up to 68% against our counterparts.

Index Terms—Handover management, multi-tier cellular networks, spectrum databases, backhaul traffic.

I. INTRODUCTION

As the first 5G network roll-outs will be upon us soon, it is expected that three main paradigms will play leading roles in achieving future traffic demands estimated to be between 100–1000× the capacity of current 4G networks: network densification, use of higher frequency bands, and spectral efficiency enhancement techniques [1]. What’s more, during the second half of the past century, wireless network performance increased by roughly 1 million times, of which up to a 2700-fold increase is due to network densification [2].

However, network densification comes associated with challenges such as network deployment, backhauling, or mobility management. According to [2], backhaul provision is one of the most critical problems when deploying small cells given the capital expenditure and operational expenditure required.

A significant shift from wireless to wired backhaul solutions is envisioned as the network densification increases. At the same time, poor mobility management could bury all the prospective gains if it is not handled appropriately, e.g., handovers (HO).

The main contributions of this paper are two-fold. First, we gauge the mobile backhaul traffic for different HO-skipping techniques found in the literature and our spectrum database-aided HO-skipping technique that exploits geolocation-awareness. Second, we have employed a realistic 5G-ready environment concerning network deployment and mobility traces to show the suitability of the proposed technique. The remainder of this paper is organised as follows: Section II gives an overview on the state of the art in the area of handover-skipping strategies for 5G, Section III discusses the system model, Section IV introduces the proposed HO skipping strategy, Section V presents the evaluation metrics, Section VI discusses simulation results, and Section VII states the conclusion as well as provides design insights.

II. RELATED WORKS

HO is the process by which a user transfers from its serving cell to a target one. It is typically associated with the best connection available, but the association might be determined by other criteria such as load, delay or user speed. For instance, the Long-Term Evolution (LTE) implements a hard HO approach that supports a wide range of association rules, known as events [3]. The LTE HO process consists of four phases: measurement, filtering, preparation, and execution. The first two take place at the user side; then, according to the event entry condition, users send a measurement report. Once the serving cell receives this report, it starts the preparation stage exchanging signalling with the target cell. During the execution phase, users are disconnected from the network before reattaching to the target cell.

In addition, HOs become more frequent as network density intensifies, shrinking base stations’ (BS) footprints, as well as user speed increases [4]. That is the main reason why several

works have pointed out the necessity of skipping HOs, to find a balance between the benefit of smaller cells but also considering disconnections as a penalty [5]–[7]. In [6], they propose the best-connected (BC) strategy, the femto-skipping (FS) strategy, and the femto-skipping with interference cancellation (FS-IC) strategy, among others. In the first algorithm, BC, users always connect to the strongest cell. Without loss of generality, we do not consider biasing. In the second and the third algorithms, FS and FS-IC, users skip femtocells alternatively along their trajectory. The skipping pursues reducing the HO rate, i.e., disconnection time for the users. When a user skips a femtocell, the second and the third strongest cells do cooperate (coordinated multipoint, CoMP [8]), intra- or inter-tier. Since the interference from the skipped femtocell, the strongest one, might be overwhelming, interference cancellation (IC) is also enabled [9].

The same authors extend their work in [6], where they propose adding location awareness to the skipping decision. In the location-aware with IC (LA) strategy, users skip any cell if the distance between the user and the target cell is above a threshold. Once an HO is skipped, both CoMP and IC are assumed following the same principles as FS-IC. However, the authors point out that estimating the user trajectory is challenging and might diminish the performance gains. That is why we have included the LA with geolocation errors (LA-GPS) strategy in the results section.

Similarly, the authors in [7] study an HO skipping technique based on the upcoming BS’s topology and a cooperative scheme based on the BSs of three consecutive cells in the user’s trajectory. In the first technique, HOs are skipped according to three different criteria: the area of the cell, the chord length of the cell, or the distance from the cell edge. The threshold is set as a factor of the expected value of each criterion. In the cooperative scheme, the users are always served by the two closest BSs in the network. Although the user side favours from these HO skipping techniques, it is not clear how the network side is affected by them. In [10], the authors conclude that ultra-dense 5G networks are not only interference-limited, but also density-limited, meaning that, as the density of small cells per macrocell increase, the backhaul network capacity will decrease. We propose an alternative HO-skipping approach whose aim is to reduce disconnections but also minimise backhaul load.

III. SYSTEM MODEL

We consider the Madrid grid model from the Mobile and wireless communications Enablers for the Twenty-twenty Information Society 5G (METIS) project [11] for our simulations. Total dimensions for Madrid grid are 387 m (west-east) and 552 m (north-south), however, to limit border effects, a wrap-around of 9 identical copies is considered.

A. Deployment

There is an orthogonal deployment of picocells complementing the macrocell tier. There is only one macro site with three sectors on the edge of a building top, and there are

also 12 pico cells installed on lampposts. Their locations are indicated in Fig. 1 while their parameters are summarised in Table I.

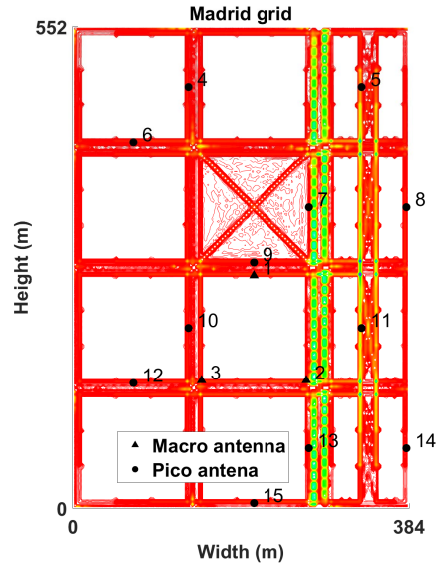


Fig. 1. Deployment for Madrid grid with a heatmap of the mobility traces.

TABLE I
DEPLOYMENT PARAMETERS

	Macro	Pico
Carrier frequency [MHz]	800	2600
Bandwidth [MHz]	20	80
Maximum Tx power (per 10 MHz) [dBm]	43	30
Antenna height [m]	52.5	10
Antenna configuration	4 TX/RX MIMO	2 TX/RX MIMO
Antenna type	Sector	Omnidirectional
Azimuth from x-axis [°]	{90, 330, 210}	-
Mechanical tilt [°]	{7, 18, 18}	-
Map resolution [m]	3	3

B. Mobility Model

Mobility traces have been generated with the open source, microscopic, and continuous road agent-based traffic simulation package *Simulation of Urban MObility* (SUMO) developed by the Institute of Transportation Systems at the German Aerospace Center [12]. It allows modelling with high detail road traffic and pedestrians too. METIS provides a publicly available, generous dataset of traces whose parameters are collected in Table II.

IV. SPECTRUM DATABASES FOR HANDOVER SKIPPING

Our proposed HO skipping technique relies on a spectrum database, also known as radio-environment maps (REM), which is primarily a database that stores spectrum information. Spectrum databases have been extensively used for spectrum sharing in television white spaces (TVWS), and their integration within an LTE network has been discussed

TABLE II
MOBILITY MODEL PARAMETERS

	Cars	Buses	Pedestrians
Dimensions [m]	1.8×4.3	12×2.5	-
Maximum speed [km/h]	50	50	3
Acceleration [m/s ²]	2.9	1.2	-
Deceleration [m/s ²]	7.5	4	-
Minimum gap [m]	2.5	4	-
Number of traces	420	320	1500
Time [s]	3600	43–135	600
Trace resolution [s]	1	1	1

in [13]. In [14], the authors create spectrum databases via an urban electromagnetic wave propagation model intended for radio planning, which predicts the field strength within 5–8 dB root-mean-square error (RMSE). In his PhD dissertation, Sato [15] focuses on measurement-based spectrum databases using Kriging interpolation. Over the course of three months, he found a correlation of roughly 0.94 in a 10-m-resolution map of a suburban area with the 90th percentile of the residual error around 7 dB. In both these works, maps are generated with similar errors that follow a log-normal distribution with zero mean for each point. In our simulations, we assume that the ray-tracing based path-loss maps provided by METIS [11] are the ground truth, thus we calculate HOs based on them. On the contrary, our radio-environment maps have been created by taking these maps and adding errors to mimic the limitations of the current methods.

A. REM-based HO Strategy

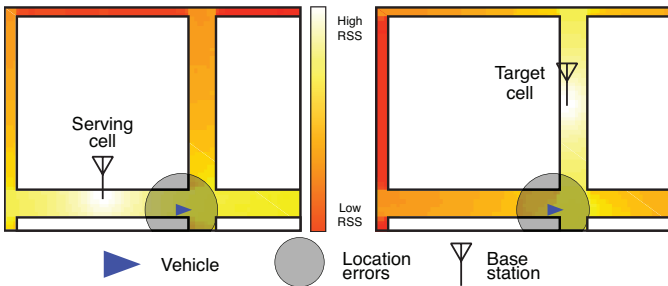


Fig. 2. A vehicle going through a city. Even though the target cell seems like a good choice, the trajectory indicates to us that it is not. Thanks to the REM, we avoid it. The circle represents the location errors.

The first two steps of our proposed algorithm REM-HO [16] are identical to LTE HO process. When users send a measurement report to start the preparation stage, they also piggyback their location and velocity (not just speed) information. This extra traffic can be quantified in 32 bytes: longitude, latitude, and the velocity vector (4 doubles). This amount of data is much smaller than the user data, and its effect on the overall traffic is negligible as the exchange of channel-state information in CoMP [17]. Consider \mathbf{x} and \mathbf{v} to be the location and the velocity of a user when reporting, respectively. We can predict the user's position assuming that the user does not change their trajectory abruptly, for example, cars and public

transport. Although pedestrians may be unpredictable, inherent location errors are more prominent. Then, we can write the predicted location \mathbf{x}_p as,

$$\mathbf{x}_p = \mathbf{x} + \mathbf{v} \times \Delta t + \varepsilon \quad (1)$$

where $\Delta t = L/|\mathbf{v}|$ is the prediction time and is chosen adaptively according to a threshold L as in [6], and to the user speed (magnitude of \mathbf{v}). We assume that location errors ε follow a bivariate normal distribution like Global Positioning System (GPS [18]). It might be argued that the velocity is also prone to errors, nonetheless, the time correlation between samples when determining the velocity cancels the error, resulting in a more reliable estimation [19].

During the signalling exchange, the predicted location is plugged into both the serving cell's spectrum database and the target cell's spectrum database to extract the predicted received signal strengths (RSS) from each cell. The HO is skipped with no collaboration between cells whatsoever, if and only if the predicted RSS from the target cell is above the predicted RSS from the serving cell,

$$\text{RSS}_{\text{target}}(\mathbf{x}_p) > \text{RSS}_{\text{serving}}(\mathbf{x}_p). \quad (2)$$

This way we ensure that the upcoming HO is worth doing since the sojourn time in the new cell will be at least Δt . We exploit not only the location of the user but also the trajectory as shown in Fig. 2, where we show the spectrum databases of the serving cell (left) and the target cell (right), respectively. For example, a user is in a vehicle going through a city, and it measures a target cell at an intersection due to the street canyon effect. If we only checked the distance, it would seem a good choice. However, if the vehicle keeps driving straight, the burden is two-fold: there are two HOs with their corresponding disconnections impacting negatively on the quality of experience (QoE) and BSs need to send data over the backhaul.

V. HANDOVER COST AND BACKHAUL TRAFFIC ESTIMATION

In this section, we present evaluation metrics that will be discussed in the results section. The first one is meant for the user side and represents the normalised average time disconnected from the network as defined in [5]. The HO cost \mathcal{D} for K tiers, which is 2 in our case, is described as

$$\mathcal{D} = \sum_i^K \sum_j^K H_{ij} \times d_{ij} \quad (3)$$

where H_{ij} represents the HO rate between tiers i and j , and d_{ij} denotes the delay associated with the type of HO. For instance, the delay incurred by a macro-macro HO is shorter than a macro-pico HO since the backhaul connection of macrocells is usually fibre optic, whereas picocells are not. Hence, for the METIS dataset, it can be further simplified to

$$\mathcal{D}^{sch} = H_{mm}^{sch} \times d_m + (H_{mp}^{sch} + H_{pp}^{sch}) \times d_p \quad (4)$$

where the subscript m means macro, p pico, and the superscript sch alludes to the HO strategy followed. We do

not distinguish the HO order, i.e., we have merged handover from/to a macro cell to/from a picocell in H_{mp} because the associated delay is the same.

The second one quantifies both upstream and downstream backhaul traffic whether using CoMP or not. LTE has two logical interfaces: S1 and X2. The S1 interface is a star network that links the advanced gateway with each cell and carries the sum of all user data, whereas the X2 interface is a mesh network that enables signalling exchange among cells. Traffic on the X2 interface remains smaller than S1 traffic unless cooperation is allowed because downlink data to one single user must be simultaneously transmitted over several links (joint-transmission CoMP [8]). Inspired by [17], S1 traffic is given by

$$S1^{sch} = \sum_M \eta(M) \times B(M) \times \rho^{sch}(M) \quad (5)$$

where $\eta(M)$ denotes the transmission mode spectral efficiency, $B(M)$ the transmission mode bandwidth, and $\rho^{sch}(M)$ the transmission mode probability that depends on the HO strategy. We define transmission mode as macrocell, picocell, and two cells in cooperation (macro-macro, pico-pico, or macro-pico). Overhead, due to tunnelling protocols and HO events, is estimated at 14% [17], then X2 upstream traffic can be written as

$$X2_{up}^{sch} = (0.14 + \bar{x}^{sch}) \times S1^{sch} \quad (6)$$

where \bar{x}^{sch} represents the inter-site ratio, i.e., the X2 interface is only used when cells at different sites cooperate. For instance, if no cooperation is needed like in the BC strategy $\bar{x}^{BC} = 0$. Equation (6) is also the total upstream traffic considered because upstream user data are ignored.

In the downstream, X2 carries data shared by all cooperating cells and is equal to

$$X2_{down}^{sch} = (0.14 + \bar{x}^{sch}) \times \sum_M [S(M) - 1] \times \eta(M) \times B(M) \times \rho^{sch}(M) \quad (7)$$

where $S(M)$ is the transmission mode cluster size, which is limited to 1 or 2 in our case (no cooperation or cooperation). Finally, we can combine (4), (5), and (7) to express downstream traffic denoted by \mathcal{T} as

$$\mathcal{T}^{sch} = (1 - \mathcal{D}^{sch}) \times (1.1 \times S1^{sch} + X2_{down}^{sch}). \quad (8)$$

VI. NUMERICAL RESULTS

We evaluate two versions of our proposed algorithm as well as the techniques presented in Section II. The first version, REM, considers GPS errors but we have perfect knowledge of the RSS map, while the second version, REM-ERR, includes both map errors and location errors. The environment used is MATLAB, where we have processed the ray-tracing based path-loss maps provided by METIS [11] and added the maximum transmit powers in Table I, so we obtain RSS maps. After that, we have calculated spectral efficiency maps for each transmission mode $\eta(M)$ in (5). The transmission

modes are macro, pico, macro-macro, pico-pico, and macro-pico. The last three modes can be with or without IC. As a result, we have eight different 3-m resolution maps, one per transmission mode, for the spectral efficiency in the Madrid grid. The bandwidth of the cooperative modes is the minimum of the two cells that are cooperating.

The mobility traces have also been treated with MATLAB to infer the transmission mode probabilities $\rho^{sch}(M)$ in (5). We have recorded for each time sample the transmission mode using all the different strategies considered in this paper, and counted the number and type of HOs for each. We put special care in ignoring random respawns of users as HOs, e.g., when a pedestrian enters a building, they will appear at another building or metro entrance randomly at the next time sample. Then, the probabilities are calculated by dividing the amount of time in each mode over the trace simulation time and averaging for each type of user, i.e., cars, buses, or pedestrians. The inter-site ratio \bar{x} in (5) is equal to the sum of all the transmission mode probabilities that involved cooperation between sites, i.e., macro-pico and pico-pico. Note that macro-macro is intra-site cooperation. Similarly, the HO rates H_{ij} in (4) have been computed as the number of HOs divided by the trace simulation time and averaged for each type of user and HO. The rest the parameters are listed in Table III.

TABLE III
SIMULATION PARAMETERS

Name	Symbol [unit]	Value
Distance threshold [6]	L [km]	$2.56/\lambda$
BS intensity of Madrid grid	λ [km ⁻²]	70.22
Prediction time	Δt [s]	$36.44/ \mathbf{v} $
Std of GPS errors [18]	σ_{XY} [m]	12.3
RMSE of map errors [14]	σ_S [dB]	6
Macro-macro HO delay [5]	d_m [s]	0.35
Pico-related HO delay [5]	d_p [s]	$2d_m$
Simulation drops	N	1000

A. Spectral Efficiency η

When a user skips a picocell, the second and the third strongest cells do cooperate [8], intra- or inter-tier. We assume that the cells are sorted in descending order concerning their RSS ($RSS_i \geq RSS_{i+1}, \forall i$). Therefore, the signal-to-interference ratio (SIR) γ in the downlink at the user is

$$\gamma = \frac{\left| \sqrt{P_2 h_2 r_2^{-\alpha}} + \sqrt{P_3 h_3 r_3^{-\alpha}} \right|^2}{\sum_{i>3} P_i h_i r_i^{-\alpha} + P_1 h_1 r_1^{-\alpha}} \quad (9)$$

where P_i is the transmit power of cell i , and h_i and $r_i^{-\alpha}$ denote the channel gain and the path-loss gain from the i -th cell, respectively. Since the interference from the skipped cell $P_1 h_1 r_1^{-\alpha}$ (the strongest one) might be overwhelming, interference cancellation is also enabled. However, we do not assume that such cancellation is performed with probability one as [5], [6]. The success probability to the cancel the n -th strongest signal is characterised in [9] and depends on the

SIR. In particular, the success probability to cancel the first strongest signal in the rest of this paper will be equal to

$$\mathbb{P}_{s,\text{can}}(\gamma) = \frac{1}{1 + \sqrt{\gamma} \times \arctan(\sqrt{\gamma})}. \quad (10)$$

In Fig. 3, we depict the empirical CDF of the spectral efficiency for each transmission mode. Clearly, the methods that do not use interference cancellation experience lower signal-to-interference ratio (SIR), affecting their spectral efficiency negatively. Even when two macro sectors cooperate (macro-macro IC), their spectral efficiency is below 3 bps/Hz. On the contrary, cooperation between tiers (macro-pico IC) and picocells (pico-pico IC) seem like a reasonable compromise, where the spectral efficiency is reduced at the expense of reducing the total number of HOs. We can also observe that approximately 65% of the time two cells from different tiers collaborating (macro-pico IC) can achieve better spectral efficiency than one single picocell (pico).

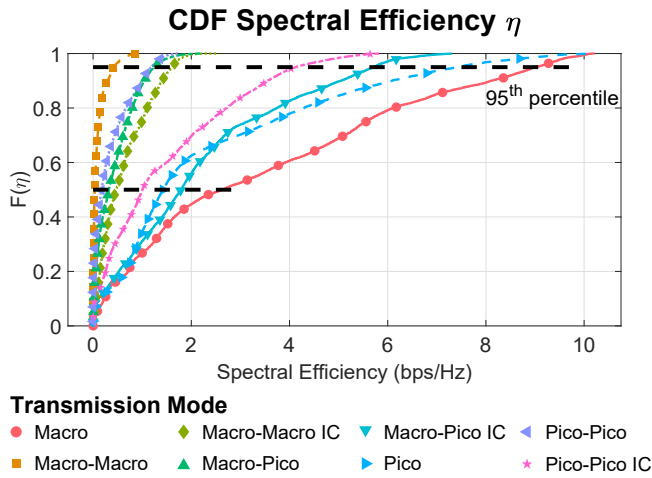


Fig. 3. Coverage probability for each transmission mode.

As recommended by the Next Generation Mobile Networks Alliance and discussed in [17], results for the mean (50th percentile) and the peak (95th percentile) spectral efficiency of joint-transmission CoMP are considered.

B. Handover Cost \mathcal{D}

In Table IV, we show the results for the HO cost (4), where we can agree that all the skipping strategies improve the baseline technique (BC). In particular, both our proposals with a reduction between 33–50% in the disconnection time are behind alternative skipping (FS and FS-IC, 40–56% reduction), and location-aware skipping (LA and LA-GPS, 56–65% reduction). This result was expected since our decision not only depended on the user’s location but also on the user’s velocity. Depending on the prediction time Δt , which changes dynamically to the current user speed, there are HOs that our strategy flags as worth doing and the other techniques skip more aggressively. Results show that location errors on average barely affect the performance of the strategies that

use location because of the nature of the errors, circularly-symmetric bivariate normal distribution.

TABLE IV
HANDOVER COST [%]

	Buses	Cars	Pedestrians
BC [5]	3.78	1.20	1.35
FS [5]	2.12	0.72	0.60
FS-IC [5]	2.12	0.72	0.60
LA [6]	1.55	0.54	0.47
LA-GPS	1.54	0.53	0.47
REM	2.30	0.80	0.67
REM-ERR	2.30	0.80	0.67

C. Backhaul Traffic

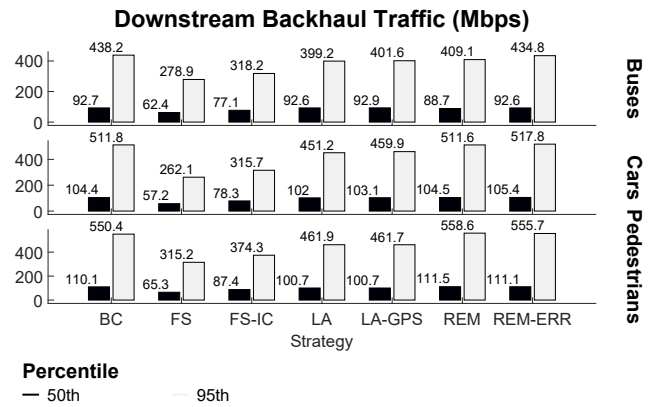


Fig. 4. Downstream backhaul traffic for 50th and 95th percentiles.

Results for the downstream backhaul traffic (8) needed for each HO skipping strategy are depicted in Fig. 4. Note that the downstream backhaul traffic is equal to the downstream user throughput, whereas the upstream backhaul traffic is just overhead due to each technique, i.e., not user data. Regarding the mean value, 50th percentile, in the downstream, it is observed that all strategies seem to perform substantially the same except for FS and FS-IC. As observed in [6], location awareness outperforms alternative skipping even when interference cancellation comes into play. This effect is even more apparent when looking at peak rates, 95th percentile. However, our technique is superior to LA and LA-GPS within 8–17% because of the extra information stored in spectrum databases. For example, LA would skip an HO when the distance is greater than a threshold blindly, but REM would check if the HO is worth in Δt seconds. This way we allow a dynamic HO skipping strategy. On top of that, LA and LA-GPS do not always succeed to cancel the main interferer following (10).

The main difference regarding traffic can be seen in the upstream backhaul traffic (6) in Fig. 5. FS, LA, and derivative methods incur in a significant 61–68% overhead increment when compared to our strategy that employs neither CoMP or SIC. Here is where the possible gains of these techniques in the downstream do not compensate for the drawbacks.

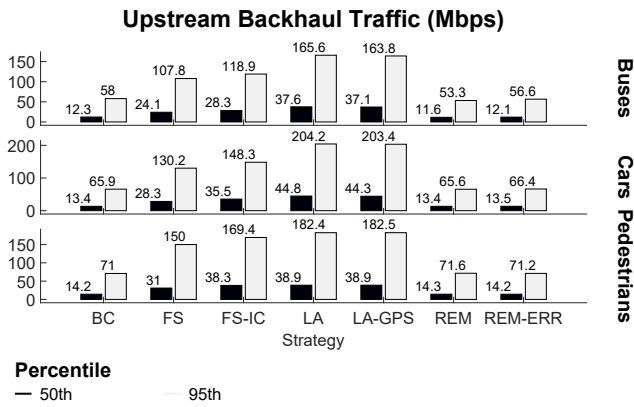


Fig. 5. Upstream backhaul traffic for 50th and 95th percentiles.

We believe that CoMP and SIC could be useful in specific scenarios, e.g., cell edge, especially when the two strongest cells cooperate. However, there are situations where, even with perfect cancellation, they are not worth it (see Fig. 3). Besides, SIC is particularly attractive for upstream and, although it is also suitable for downstream, its impact on the user autonomy is not studied [9].

VII. CONCLUSIONS

In this paper, we have compared the backhaul traffic for several handover skipping techniques in a realistic dense urban environment. We have shown that location awareness represents an improvement over the conventional handover strategy on the user side. However, on the network side, skipping strategies can introduce a decent amount of overhead at the same time. We present a low-overhead handover skipping scheme that uses spectrum databases to support measurement reports on the field. The results show that our technique finds a balance between the conventional method and other skipping strategies. Our technique does not overload the upstream, reducing in more than 61% of the required data exchange between base stations, while maintaining the same quality of service in the downstream with at least 33% less time disconnected from the network because of the handovers.

REFERENCES

- [1] J. G. Andrews, S. Buzzi, W. Choi, S. V. Hanly, A. Lozano, A. C. K. Soong, and J. C. Zhang, "What will 5G be?" *IEEE Journal on Selected Areas in Communications*, vol. 32, no. 6, pp. 1065–1082, 2014.
- [2] D. Lopez-Perez, M. Ding, H. Claussen, and A. H. Jafari, "Towards 1 Gbps/UE in cellular systems: understanding ultra-dense small cell deployments," *IEEE Communications Surveys & Tutorials*, vol. 17, no. 4, pp. 2078–2101, 2015.
- [3] D. Lopez-Perez, I. Guvenc, and X. Chu, "Mobility management challenges in 3GPP heterogeneous networks," *IEEE Communications Magazine*, vol. 50, no. 12, pp. 70–78, 2012.
- [4] W. Bao and B. Liang, "Stochastic geometric analysis of user mobility in heterogeneous wireless networks," *IEEE Journal on Selected Areas in Communications*, vol. 33, no. 10, pp. 2212–2225, 2015.
- [5] R. Arshad, H. ElSawy, S. Sorour, T. Y. Al-Naffouri, and M.-S. Alouini, "Velocity-aware handover management in two-tier cellular networks," *IEEE Transactions on Wireless Communications*, vol. 16, no. 3, pp. 1851–1867, 2017.

- [6] R. Arshad, H. ElSawy, S. Sorour, T. Y. Al-Naffouri, and M.-S. Alouini, "Handover management in 5G and beyond: a topology aware skipping approach," *IEEE Access*, vol. 4, pp. 9073–9081, 2016.
- [7] E. Demarchou, C. Psomas, and I. Krikidis, "Mobility Management in Ultra-Dense Networks: Handover Skipping Techniques," *IEEE Access*, vol. 6, pp. 11 921–11 930, 2018.
- [8] R. Irmer, H. Droste, P. Marsch, M. Grieger, G. Fettweis, S. Brueck, H.-P. Mayer, L. Thiele, and V. Jungnickel, "Coordinated multipoint: concepts, performance, and field trial results," *IEEE Communications Magazine*, vol. 49, no. 2, pp. 102–111, 2011.
- [9] M. Wildemeersch, T. Q. S. Quek, M. Kountouris, A. Rabbachin, and C. H. Slump, "Successive interference cancellation in heterogeneous networks," *IEEE Transactions on Communications*, vol. 62, no. 12, pp. 4440–4453, 2014.
- [10] X. Ge, S. Tu, G. Mao, C. Wang, and T. Han, "5G Ultra-Dense Cellular Networks," *IEEE Wireless Communications*, vol. 23, no. 1, pp. 72–79, February 2016.
- [11] Mobile and wireless communications Enablers for Twenty-twenty Information Society-II, "Performance evaluation framework," Deliverable (D) 2.1, 2016.
- [12] D. Krajzewicz, J. Erdmann, M. Behrisch, and L. Bieker, "Recent development and applications of SUMO-Simulation of Urban MObility," *International Journal On Advances in Systems and Measurements*, vol. 5, no. 3&4, 2012.
- [13] J. Perez-Romero, A. Zalonis, L. Boukhatem, A. Kliks, K. Koutlia, N. Dimitriou, and R. Kurda, "On the use of radio environment maps for interference management in heterogeneous networks," *IEEE Communications Magazine*, vol. 53, no. 8, pp. 184–191, 2015.
- [14] Y. Corre and Y. Lohan, "Three-dimensional urban EM wave propagation model for radio network planning and optimization over large areas," *IEEE Transactions on Vehicular Technology*, vol. 58, no. 7, pp. 3112–3123, 2009.
- [15] K. Sato, "Measurement-based spectrum database for spatial spectrum sharing," PhD, 2017.
- [16] C. Suarez-Rodriguez, B. A. Jayawickrama, F. Bader, E. Dutkiewicz, and M. Heimlich, "REM-based handover algorithm for next-generation multi-tier cellular networks," in *2018 IEEE Wireless Communications and Networking Conference (WCNC)*, Conference Proceedings, pp. 1–6.
- [17] V. Jungnickel, S. Jaeckel, K. Brner, M. Schlosser, and L. Thiele, "Estimating the mobile backhaul traffic in distributed coordinated multipoint systems," in *2012 IEEE Wireless Communications and Networking Conference (WCNC)*, Conference Proceedings, pp. 3763–3768.
- [18] T. O. of the Secretary of Defense (U.S. government), "GPS Standard Positioning Service (SPS) performance standard," U.S. government, Standard (S), 2008.
- [19] P. Ranacher, R. Brunauer, W. Trutschig, S. Van der Spek, and S. Reich, "Why GPS makes distances bigger than they are," *International Journal of Geographical Information Science*, vol. 30, no. 2, pp. 316–333, 2016.